

Real-Time Precise Point Positioning in NAD83: Global and Regional Broadcast Corrections Compared

P. J. G. Teunissen¹; L. Huisman²; and C. Hu, Ph.D.³

Abstract: Real-time precise point positioning (PPP) is possible through the availability of the real-time satellite orbit and clock corrections to broadcast ephemeris, the real-time broadcast corrections (BCs). The real-time BCs are currently available in global as well as in regional reference frames. In this contribution, PPP usage and the performance of these global and regional BCs are analyzed for the North American Datum of 1983 (NAD83). The limitations of the current regional BC approach for NAD83 are identified and the coordinate differences it leads to compared with the traditional global BC approach are shown. Although the biases as a result of the different reference frame usage are shown to be subcentimeter, it is also shown how they can be reduced or eliminated by modifying either the PPP algorithm or the regional BC approach. Analyses were performed for three different PPP variants, a single-frequency ionosphere-free variant, a dual-frequency ionosphere-free variant, and a single-frequency ionosphere-corrected variant. DOI: 10.1061/(ASCE)SU.1943-5428.0000089. © 2013 American Society of Civil Engineers.

CE Database subject headings: Global positioning systems; Surveys; Satellites.

Author keywords: Global positioning system; Precise point positioning; ITRF; NAD83; Global and regional broadcast corrections.

Introduction

Precise point positioning (PPP) is a global positioning system (GPS) positioning method that processes undifferenced pseudorange and carrier phase measurements from a stand-alone GPS receiver to compute positions with high decimeter or centimeter accuracy everywhere on the globe (Zumberge et al. 1997; Kouba and Heroux 2001; Ovstedal 2002). In recent years, services have been developed that allow high-accuracy ephemeris data to be made available in real time to users (CODE 2006; Kouba 2003; Tetreault et al. 2005; BKG 2010). Such availability has created, and will continue to create, a wide range of PPP applications (Heroux et al. 2004; Bisnath and Gao 2008). Important examples of such services are the real-time (RT) GPS satellite orbit and clock corrections to broadcast ephemeris (Sohne et al. 2008). These RT broadcast corrections (BCs) provide users with precise orbit and clock corrections as needed for PPP. The BCs are not only available in a global reference frame (GRF) but are also in a selected set of regional reference frames (RRFs), such as the North American Datum (NAD) of 1983 (NAD83) (BKG 2010; Sohne 2010). In this contribution, the usage of these NAD83 regional BCs (RBCs) for single- and dual-frequency PPP is analyzed for the first time and their performance with the usage of the more traditional global BCs (GBCs) is compared.

The rationale behind the RBCs is the thought that when processing stand-alone GPS data the reference frame in which the user's position is obtained is defined by the realization of the reference system in which the satellite positions are given. Therefore, it has been indicated in the literature that the GRF-to-RRF transformation of satellite trajectories is a useful alternative to the GRF-to-RRF transformation of station coordinates because it potentially simplifies access to the RRF by allowing users to work exclusively in a nonglobal regional datum (Craymer et al. 2000; Kouba 2002; Craymer 2006; Schwarz 1989).

This contribution is organized as follows. To be able to evaluate the role played in PPP by the reference frames, a brief description of the NAD83 and the International Terrestrial Reference Frame (ITRF), and their ellipsoidal coordinate differences, is given in the subsequent section. Then, the GBC and RBC approaches for single- and dual-frequency PPP in NAD83 are analyzed and compared. The limitations of the current RBC approach are identified and the coordinate differences they lead to with respect to the GBC approach are shown. Next, it is shown how to modify either the PPP algorithm or the RBC approach such that consistency among the two approaches is restored. Because the identified limitations of the PPP RBC approach are inherent as a result of different reference frame usage, the results of this contribution are in support of the plan to replace NAD83 by 2018 with a new geometric datum that removes the disagreements with the ITRF (NOAA 2008).

¹Professor and ARC Federation Fellow, GNSS Research Centre, Curtin Univ. of Technology, Kent St., Perth 6152, Australia; and Delft Institute of Earth Observation and Space Systems (DEOS), Delft Univ. of Technology, 2600 GB Delft, Netherlands (corresponding author). E-mail: p.teunissen@curtin.edu.au

²Research Fellow, GNSS Research Centre, Curtin Univ. of Technology, Kent St., Perth 6152, Australia.

³Research Fellow, GNSS Research Centre, Curtin Univ. of Technology, Kent St., Perth 6152, Australia.

Note. This manuscript was submitted on January 18, 2012; approved on May 24, 2012; published online on May 29, 2012. Discussion period open until July 1, 2013; separate discussions must be submitted for individual papers. This paper is part of the *Journal of Surveying Engineering*, Vol. 139, No. 1, February 1, 2013. ©ASCE, ISSN 0733-9453/2013/1-1-10/\$25.00.

NAD83 and ITRF

For proper usage of PPP BCs it is important to understand the role played by the reference frames. Therefore, in this section the NAD83, its transformational link to the ITRF, and the effect this transformation has on the location-dependent ellipsoidal coordinate differences between the two frames are briefly described.

North American Datum 1983

The adopted datum or reference system for spatial positioning in the United States and Canada is NAD83. For a detailed description

of its definition, establishment, and evolution, the reader is referred to Schwarz (1989), Snay and Soler (2000a, b), Soler and Snay (2004), Craymer et al. (2000), and Craymer (2006). The first realization of NAD83, which relied heavily on Doppler satellite observations, was adopted in 1986 by the U.S. National Geodetic Survey (NGS). It is referred to as NAD83 (1986). Since then, the NAD has undergone another five realizations in the United States, the last one being NAD83 (CORS96). For this realization, the NAD83 was precisely linked to the ITRF, which is the best realization of a geocentric coordinate system (Boucher and Altamimi 1996). For that purpose, the NGS and Natural Resources Canada (NRCAN) determined the ITRF96-NAD83 transformation parameters from the positional coordinates of 12 selected very-long baseline interferometry (VLBI) stations in the two frames. To establish the NAD83(CORS96) realization, the estimated ITRF96-NAD83 transformation was subsequently used to compute NAD83 coordinates for all the then-existing GPS CORS.

Following a reanalysis of CORS data and the recent change of the reference frame in which the International GPS Service (IGS) products are given (IGS08 instead of IGS05, since April 17, 2011; IGS05 and IGS08 are IGS realizations of ITRF05 and ITRF08) (Reischung et al. 2011), the NGS has recently released an updated realization of NAD83, NAD83(2011) (NOAA 2011). The definition of the origin, scale, and rotation of NAD83(2011) remains the same as for NAD83(CORS96); however, factors such as a longer GPS time series, the improved IGS08 GRF, and better processing algorithms have resulted in improved NAD83 coordinates for CORS sites.

At the time of its first realization, NAD83 was intended to be a geocentric system and was compatible with the other geocentric systems of the time, such as the original realization of the World Geodetic System 1984 (WGS84). However, because of the later use of more accurate techniques, it is known that NAD83 is offset by about 2 m from the geocenter (see also Table 1). To remove the disagreements with the ITRF, the NGS is planning to replace NAD83 with a new geometric datum by 2018 (NOAA 2008). The primary means of accessing this datum will be global navigation satellite system (GNSS) technology. The new geometric datum will be defined in conjunction with a new geopotential datum. However, it is not yet known whether the new geometric datum will be fixed to the stable North American plate. The exact definition of the new geometric datum will be determined in the years to come through a series of stakeholder feedback forums (NOAA 2008).

Table 1. Transformation Parameters from ITRF2005 to NAD83 (Second Column) and IGS08 to NAD83 (Third Column)

t_0 (year) = 1,997.0	ITRF2005	IGS08
$d_x(t_0)$ (mm)	996.3	993.43
$d_y(t_0)$ (mm)	-1,902.4	-1,903.31
$d_z(t_0)$ (mm)	-521.9	-526.55
$r_x(t_0)$ (mas)	-25.915	-25.91467
$r_y(t_0)$ (mas)	-9.426	-9.42645
$r_z(t_0)$ (mas)	-11.599	-11.59935
$\Delta s(t_0)$ (ppb)	0.78	0.71504
\dot{d}_x (mm/year)	0.5	0.79
\dot{d}_y (mm/year)	-0.6	-0.60
\dot{d}_z (mm/year)	-1.3	-1.34
\dot{r}_x (mas/year)	-0.067	-0.06667
\dot{r}_y (mas/year)	0.757	0.75744
\dot{r}_z (mas/year)	0.051	0.05133
$\Delta \dot{s}$ (ppb/year)	-0.10	-0.10201

Note: mas = milliarcsec and ppb = part per billion.

ITRF-to-NAD83 Transformation

In contrast to NAD83, which is defined such that all points on the North American plate located sufficiently far from the plate boundary zone have, on average, zero horizontal velocities, the ITRF (Altamimi et al. 2007) is dynamic and its coordinates change primarily to account for tectonic processes. The organization responsible for maintaining the ITRF is the International Earth Rotation and Reference Systems Service (IERS). Since the introduction of the ITRF96-NAD83 transformation, several newer ITRF realizations were introduced by the IERS. As the available RT NAD83 RBCs are based on the ITRF2005-to-NAD83 transformation (BKG 2010), the subsequent analysis will be based on this transformation as well.

The ITRF-to-NAD83 coordinate transformation at an epoch t is performed by a seven-parameter similarity transformation as follows (Soler and Marshall 2003; Soler and Snay 2004):

$$\mathbf{x}_{\text{NAD83}}(t) = s(t) \mathbf{R}(t) \mathbf{x}_{\text{ITRF}}(t) + \mathbf{d}(t) \quad (1)$$

where

$$s(t) = [1 + \Delta s(t)]$$

$$\mathbf{R}(t) = \begin{bmatrix} 1 & -r_z(t) & r_y(t) \\ r_z(t) & 1 & -r_x(t) \\ -r_y(t) & r_x(t) & 1 \end{bmatrix}$$

$$\mathbf{d}(t) = [d_x(t), d_y(t), d_z(t)]^T$$

where \mathbf{x}_{ITRF} = coordinate vector in the global ITRF frame; $\mathbf{x}_{\text{NAD83}}$ = coordinate vector in the regional NAD83 frame; s = scale factor with increment Δs ; \mathbf{R} = matrix with differential rotation angles r_x , r_y , and r_z ; and \mathbf{d} = translation vector.

Because the seven transformation parameters are considered to change linearly with time, transformation (1) can be computed for any epoch t once the seven similarity transformation parameters [$s(t_0)$, $\mathbf{R}(t_0)$, $\mathbf{d}(t_0)$], plus their seven time rates of change (\dot{s} , $\dot{\mathbf{R}}$, $\dot{\mathbf{d}}$), are given at a certain reference epoch t_0 . These 14 parameters are then used to compute the seven similarity transformation parameters for any epoch t as

$$s(t) = s(t_0) + \dot{s}(t - t_0)$$

$$\mathbf{R}(t) = \mathbf{R}(t_0) + \dot{\mathbf{R}}(t - t_0) \quad (2)$$

$$\mathbf{d}(t) = \mathbf{d}(t_0) + \dot{\mathbf{d}}(t - t_0)$$

The NGS-adopted values of these 14 parameters are given in Table 1 for both the ITRF2005-to-NAD83(CORS96) transformation [adopted from Pearson et al. (2010) and Craymer (2006)] and the IGS08-to-NAD83(2011) transformation [adopted from NOAA (2011)]. The relatively large rotational rates are a result of the North American plate rotations and make NAD83 fixed to the North American plate. The rotation matrix of Eq. (1) and its corresponding entries in Table 1 are given according to the IERS conventions (Petit and Luzum 2010). The same definition is used in Craymer (2006); however, a different definition is used in Pearson et al. (2010), which results in a change of the sign in the rotation parameters and their rates.

From Table 1 it can be seen that the differences in transformation parameters between the ITRF2005-to-NAD83(CORS96) transformation and the IGS08-to-NAD83(2011) transformation are small; the largest difference being in the scale. In the computations NAD83 (CORS96) was used because it is the same realization in which the BCs are available. However, NAD83(2011) was included in the analysis and conclusions as well.

Effect of Scale, Rotation, and Translation

The effect on the position coordinates of the ITRF-NAD83 transformation will vary from location to location. For the purpose of the PPP analyses, this location-dependent effect in terms of ellipsoidal coordinates is evaluated.

Starting from Eq. (1) and writing \mathbf{x} instead of \mathbf{x}_{ITRF} , yields with $s = 1 + \Delta s$, $\mathbf{R} = \mathbf{I} + \Delta \mathbf{R}$, when neglecting second- and higher-order terms

$$\mathbf{x}_{\text{NAD83}} = (1 + \Delta s)(\mathbf{I} + \Delta \mathbf{R})\mathbf{x} + \mathbf{d} = \mathbf{x} + \Delta s\mathbf{x} + \Delta \mathbf{R}\mathbf{x} + \mathbf{d} \quad (3)$$

and thus with $\Delta \mathbf{x}_{\text{NAD83}} = \mathbf{x}_{\text{NAD83}} - \mathbf{x}$

$$\Delta \mathbf{x}_{\text{NAD83}} = \Delta s\mathbf{x} + \mathbf{r} \times \mathbf{x} + \mathbf{d} \quad (4)$$

where the vector product form $\Delta \mathbf{R}\mathbf{x} = \mathbf{r} \times \mathbf{x}$ is used, with $\mathbf{r} = [r_x, r_y, r_z]^T$.

To formulate expression (4) in terms of ellipsoidal coordinates ϕ , λ , and h the following equation is used:

$$\begin{bmatrix} x \\ y \\ z \end{bmatrix} = \begin{bmatrix} (N + h)\cos\phi\cos\lambda \\ (N + h)\cos\phi\sin\lambda \\ [N(1 - e^2) + h]\sin\phi \end{bmatrix} \quad (5)$$

where N = east-west radii of curvature and e = eccentricity. Linearizing and then inverting Eq. (5) gives

$$\begin{bmatrix} \Delta h \\ (M + h)\Delta\phi \\ (N + h)\cos\phi\Delta\lambda \end{bmatrix} = \mathbf{R}(\phi, \lambda) \begin{bmatrix} \Delta x \\ \Delta y \\ \Delta z \end{bmatrix} \quad (6)$$

with orthogonal matrix

$$\mathbf{R}(\phi, \lambda) = \begin{bmatrix} \cos\phi\cos\lambda & \cos\phi\sin\lambda & \sin\phi \\ -\sin\phi\cos\lambda & -\sin\phi\sin\lambda & \cos\phi \\ -\sin\lambda & \cos\lambda & 0 \end{bmatrix} \quad (7)$$

where M = north-south radii of curvature.

Substituting Eq. (4) into Eq. (6) then finally gives

$$\begin{bmatrix} \Delta h \\ (M + h)\Delta\phi \\ (N + h)\cos\phi\Delta\lambda \end{bmatrix} = \mathbf{R}(\phi, \lambda)[\Delta s\mathbf{x} + \Delta \mathbf{R}\mathbf{x} + \mathbf{d}] \\ = \Delta s\mathbf{u} + \boldsymbol{\omega} \times \mathbf{u} + \boldsymbol{\delta} \quad (8)$$

where $\mathbf{u} = \mathbf{R}(\phi, \lambda)\mathbf{x}$, $\boldsymbol{\omega} = \mathbf{R}(\phi, \lambda)\mathbf{r}$, and $\boldsymbol{\delta} = \mathbf{R}(\phi, \lambda)\mathbf{d}$.

Expression (8) shows how the NAD83-ITRF north-east-up (N-E-U) coordinate differences are affected by differential scale Δs , differential rotation $\boldsymbol{\omega} \times$, and translation $\boldsymbol{\delta}$. Together with the North American digital terrain model (Pavlis et al. 2006), the values of these coordinate differences and their variability are graphically displayed in Fig. 1 for the continental United States. The horizontal coordinate differences, which can be as large as a few meters, are driven by translation and rotation (the effect of scale is here less than 1 mm). The height differences range from about -0.25 m in the north-west to 1.65 m in the south-east. Because the combined effect of rotation and scale can be shown here to be only at the few-mm level, the height differences are primarily a result of the non-geocentricity of NAD83; i.e., the translation $\boldsymbol{\delta}$ in Eq. (8).

PPP in NAD83

In this section the two approaches that are currently available for realizing RT PPP in NAD83 are described. The two approaches are compared and evaluated using GPS data from a set of eight, evenly distributed, permanent tracking stations in the continental United States.

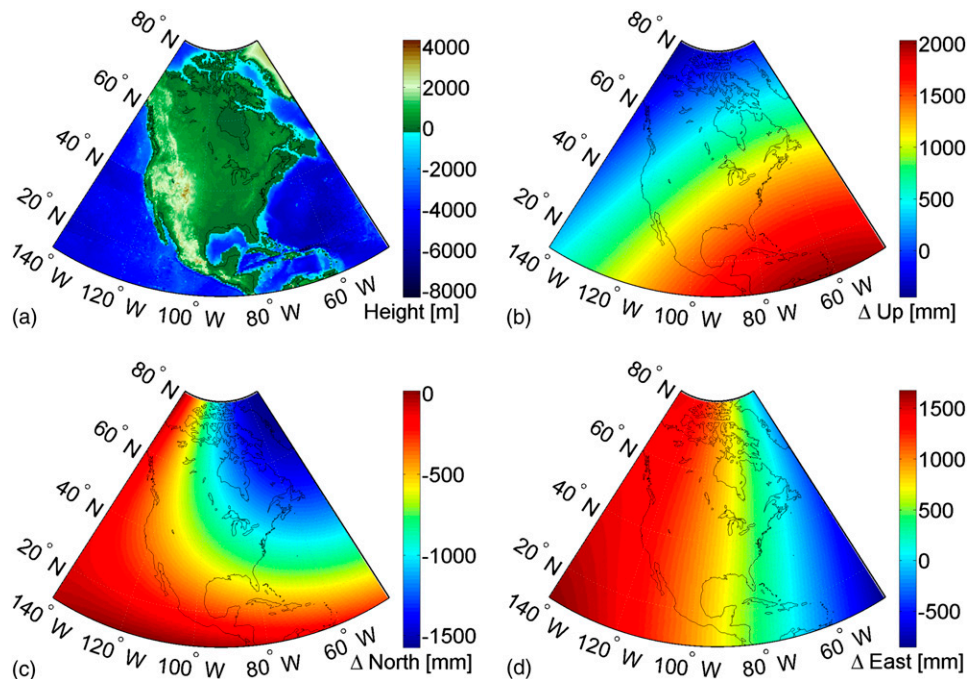


Fig. 1. (Color) North American digital terrain model: (a) derived from Global DTM2006.0 and NAD83-ITRF2005 ellipsoidal coordinate differences [Epoch Day of Year (DOY) 079, 2011] for the components (b) height, (c) north-south, and (d) east-west

Global and Regional BCs

Satellite positions are usually given in a GRF. Rather than having the user's position in a GRF, a PPP user is often interested in obtaining the final positions in a RRF, such as NAD83. To obtain the user's position in a RRF, a frame transformation has to be applied from the GRF, in which the satellite positions are given to the RRF.

Currently, a user can follow two different approaches for determining the RRF position coordinates; i.e., the GBC approach or the RBC approach. The GBC approach is the traditional one, while the RBC approach is a relatively recent one. Although tools have been available for the RBC approach for many years (e.g., Kouba 2002), the RBC approach has become possible in real time through the RT-IGS pilot project and the European Reference Frame (EUREF) RT analysis project (EUREF-RT) (Sohne et al. 2008; Sohne 2010; BKG 2010). The RBC approach can currently be used for several RRFs, such as the NAD83 (BKG 2010). The two approaches are schematically depicted in Fig. 2.

Traditionally, the transformation from ITRF to NAD83 is applied at the user level [see Fig. 2(a)]. In this GBC approach, precise orbits and clocks [Box 1 in Fig. 2(a)] are used to generate GBCs (Box 3) to the broadcast ephemeris (Box 2). The PPP algorithm (Box 4) uses these GBCs and the broadcast ephemeris together with the GPS observations (Box 5) to compute a precise receiver position in ITRF (Box 6). An ITRF-to-NAD83 coordinate transformation (Box 7) is then finally applied to obtain the receiver position in NAD83

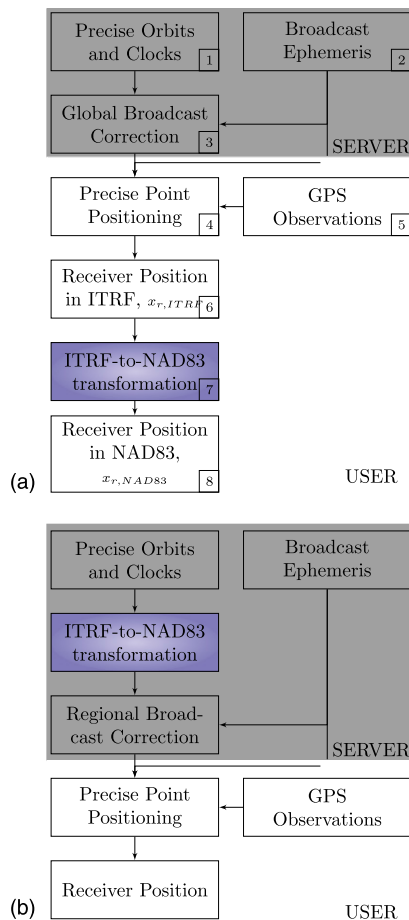


Fig. 2. Flow diagram for obtaining a PPP position in NAD83: (a) GBC approach (USER-side ITRF-to-NAD83 transformation); (b) RBC approach (SERVER-side ITRF-to-NAD83 transformation)

(Box 8). The RBC approach is depicted in Fig. 2(b). The main difference from the GBC approach is that with the RBC approach, the ITRF-to-NAD83 transformation is already performed by the server that computes the BCs rather than by the individual user. The benefit of the RBC approach is thus thought to be that the user no longer has to transform the position but will get the position directly in the desired RRF.

RT PPP in NAD83 with GBCs

The analysis was started using the GBCs for RT PPP. The PPP method, using IGS products and the necessary correction models, is described in Kouba and Heroux (2001). For handling of the ionospheric delays, various options are available. In Ovstedal (2002) and van Bree and Tiberius (2012), external information from global ionospheric maps (GIMs) (Schaer 1999) was used to correct a priori the single-frequency observations for the ionospheric delays. On the other hand, in Kouba and Heroux (2001) and Montenbruck (2003) the unknown ionospheric delays were eliminated from the observation equations by using appropriate linear combinations of the single- or the dual-frequency phase and code observations.

In the RT PPP software all three ionospheric variants have been implemented; i.e., the two ionosphere-free variants (single- and dual-frequencies) and the single-frequency, GIM-corrected variant. All three variants make use of phase and code data and solve for the real-valued ambiguities. The single-frequency ionosphere-free variant is equivalent to working with the average of the L_1 phase and code observables. In both single-frequency variants the tropospheric delay is a priori corrected for, while in the dual-frequency variant the zenith tropospheric delay (ZTD) is estimated. For the tropospheric delay the Saastamoinen model (Saastamoinen 1972a, b, 1973; Davis et al. 1985; Petit and Luzum 2010) was used, with the Ifadis mapping function (Ifadis 1992; Niell 1996), using standard atmosphere values for pressure and temperature (Kleijer 2004).

For all three variants, the kinematic PPP-NAD83 performance of the GBC approach using DLR RETICLE clock products were analyzed (Hauschild and Montenbruck 2009) for the eight U.S. stations shown in Fig. 3. The receivers and antennas of these stations are listed in Table 2. Stations BILL, AMC2, HNPT, and EPRT are IGS stations. Because the performance of the eight stations was comparable, only the kinematic PPP time series for Stations AMC2 and EPRT are shown in Figs. 4 and 5, respectively. The single- and

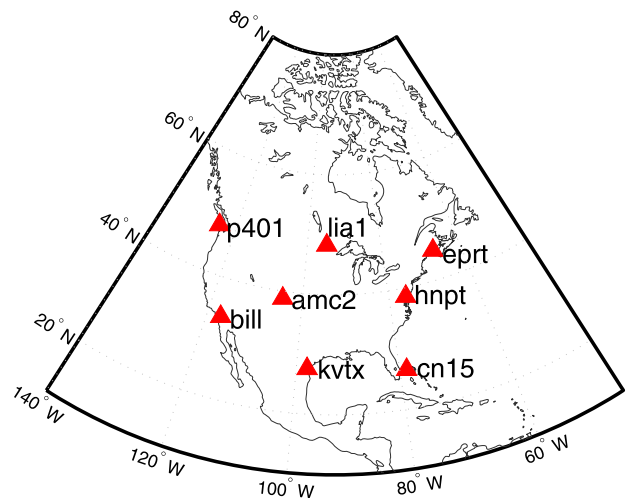


Fig. 3. Location of the eight U.S. stations

Table 2. Receiver and Antennas of the Eight U.S. Stations

Station	Receiver	Antenna	Radome
P401	Trimble NetRS	TRM29659.00	SCIT
LIA1	Trimble NetRS	TRM41249.00	NONE
EPRT	Leica GRX1200GGPRO	TRM29659.00	LEIS
BILL	Trimble NetRS	ASH701945B-M	SCIT
AMC2	Ashtech Z-XII3T	AOAD M-T	NONE
HNPT	Leica GRX1200GGPRO	LEIAX1202GG	NONE
KVTX	Trimble NetRS	TRM29659.00	SCIT
CN15	Trimble NetR9	TRM57971.00	SCIT

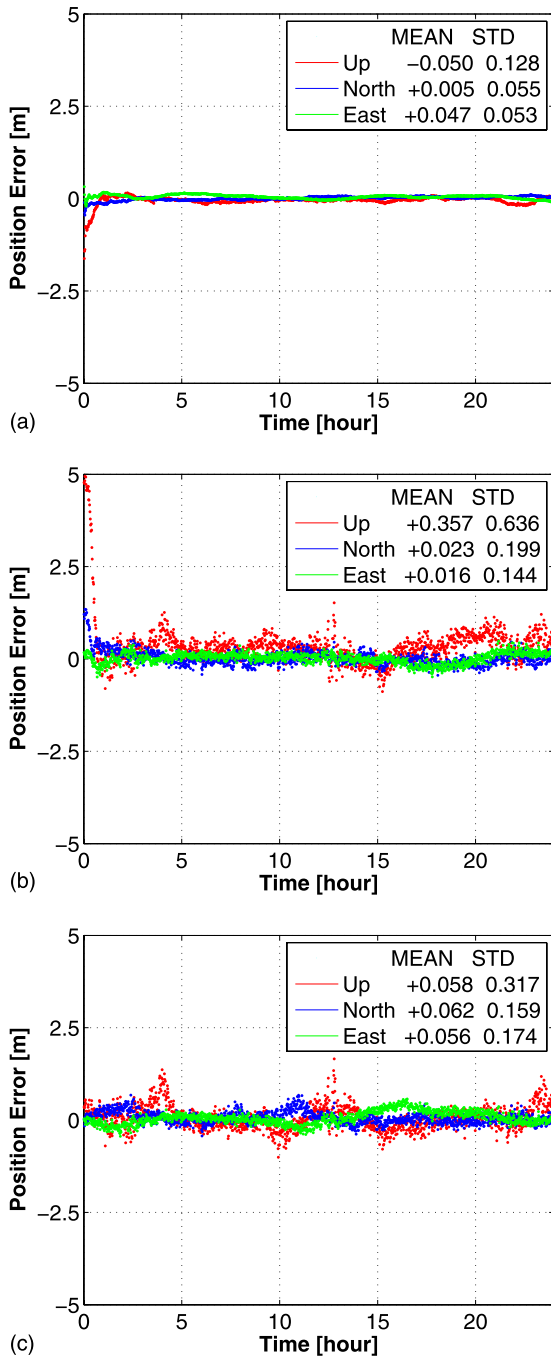


Fig. 4. (Color) N-E-U kinematic PPP time series for Station AMC2: ionosphere free and GIM corrected; (a) dual-frequency ionosphere-free; (b) single-frequency ionosphere-free; (c) single-frequency with GIM corrections

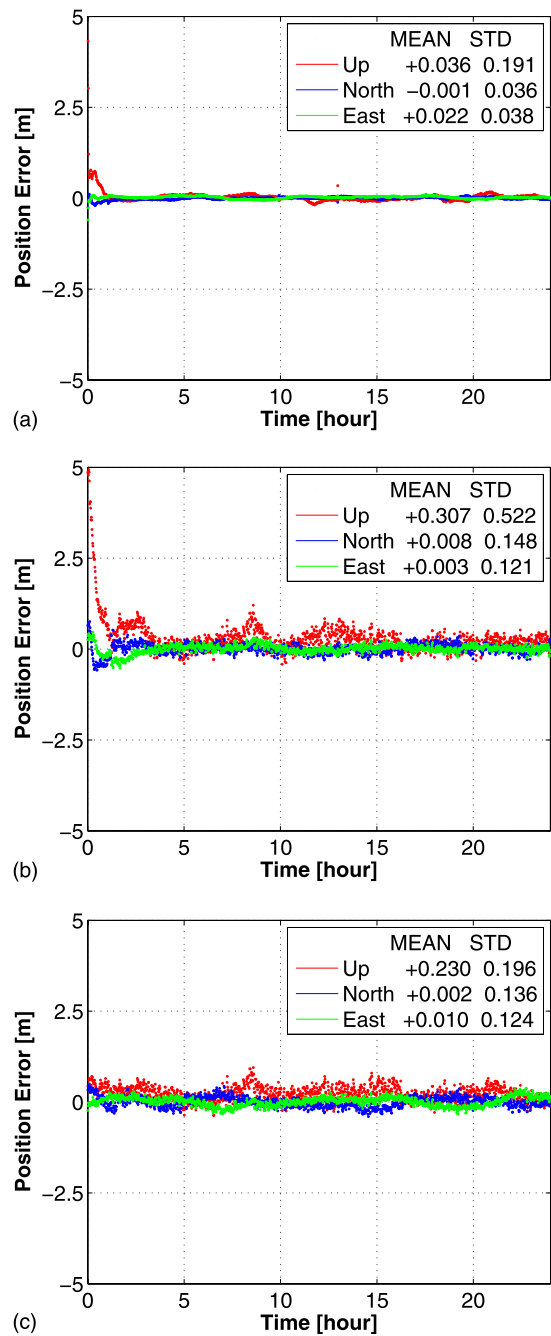


Fig. 5. (Color) N-E-U kinematic PPP time series for Station EPRT: ionosphere free and GIM corrected; (a) dual-frequency ionosphere-free; (b) single-frequency ionosphere-free; (c) single-frequency with GIM corrections

dual-frequency ionosphere-free variants have a convergence of about 1 h, whereas the single-frequency variant with GIM corrections shows little convergence time. The precision after convergence for the dual-frequency case is at subdecimeter level, while the single-frequency case achieves better than 0.5-m precision for the vertical and better than 0.2 m in the horizontal component.

RT PPP in NAD83 with RBCs

The current RT kinematic PPP results using the NAD83-RBCs are presented (Weber et al. 2007). Because the RBC approach aims at

providing a PPP-user position in the RRF, the positioning results of the two approaches, GBC and RBC, were compared at the coordinate level in the RRF, in this case NAD83. All settings of the software were identical in the PPP processing of the GBCs and the RBCs; only the BC input differed.

For all eight stations analyzed, the same conclusion could be drawn; namely, that the results obtained with the RBC approach differed from those obtained with the GBC approach. Hence, the two approaches did not give the same results. As representative for the eight stations, the results for Station AMC2 are shown. Fig. 6 shows the coordinate differences in NAD83 for both approaches. Fig. 6(a) shows the single-frequency, GIM-corrected, N-E-U differences, while Fig. 6(b) shows the dual-frequency N-E-U and ZTD differences. All components showed systematic errors that were slowly changing over time. The largest differences were found in the up component (about 4 mm in height), while the horizontal coordinate differences and the ZTD differences were much smaller.

The aforementioned shows that the RBC approach of making satellite positions directly available in a RRF (Sohne et al. 2008;

BKG 2010) does not give the PPP-user position directly in that same RRF. Hence, the originally thought of the benefit from the RBCs—namely, that a PPP user would no longer have to transform the position when using the RBC approach—is not quite correct. Although the differences with the GBC approach are small, PPP usage of the NAD83-RBCs does not provide positions in NAD83. This identified pitfall can be understood when the workings of the PPP algorithm itself are considered.

Modifying the PPP Algorithm or the RBC Approach

In this section it is shown how to modify the PPP algorithm such that consistency among the two approaches is again restored. Instead of modifying the PPP algorithm, an alternative approach is also provided.

Scale-Corrected PPP Receiver-Satellite Ranges

A closer look at the effect of the ITRF-to-NAD83 transformation on the positioning algorithm reveals that although the rotation and translation do not affect receiver-satellite ranges, the scaling of course does. Hence, identical ranges between the two approaches can only be expected if the GRF and the RRF have the same scale. Because this is not the case between ITRF2005 and NAD83 (cf. Table 1), scale-induced, time-varying receiver-satellite geometry-dependent biases are present in the RBC approach, as is shown in Fig. 6.

To correct for the previously described scale-induced biases, an appropriate modification of the phase and code observation equations in the PPP algorithm is needed. Let $\rho_{r,ITRF}^s$ and $\rho_{r,NAD}^s$ denote the receiver-satellite ranges in the ITRF and NAD83, respectively. Then, these ranges and their increments are related as

$$\begin{aligned} \rho_{r,ITRF}^s &= \|x_{ITRF}^s - x_{r,ITRF}\| \\ &= \frac{1}{s} \|x_{NAD}^s - x_{r,NAD}\| \\ &= \frac{1}{s} \rho_{r,NAD}^s \end{aligned} \quad (9)$$

and

$$\Delta \rho_{r,ITRF}^s = -\frac{1}{s} (u_{r,NAD})^T \Delta x_{r,NAD} \quad (10)$$

where x_{ITRF}^s , $x_{r,ITRF}$, x_{NAD}^s , and $x_{r,NAD}$ = satellite and receiver position vectors in ITRF and NAD83, respectively; and $u_{r,NAD}$ = unit direction vector from receiver to satellite and $\Delta x_{r,NAD}$ = increment vector of the receiver position, both expressed in NAD83.

Eqs. (9) and (10) show how the PPP observation equations need to be modified in order to obtain scale bias-free receiver-satellite ranges with the RBC approach. Fig. 7(a) depicts this change to the flow diagram and Figs. 7(b and c) show the results of processing the data using this modified approach. Fig. 7(b) shows the single-frequency N-E-U differences between using the GBC approach and the modified range-corrected RBC approach, while Fig. 7(c) shows the dual-frequency N-E-U and ZTD differences between using these two approaches. As the results show, the biases have been reduced. For the dual-frequency case, the biases are practically absent, while for the single-frequency case, the position biases have been reduced from about 4 mm in height to 1 mm in height.

Height-Corrected PPP Tropospheric Delays

Although the time series in Figs. 7(b and c) show that the differences between using the GBC approach and the modified range-corrected

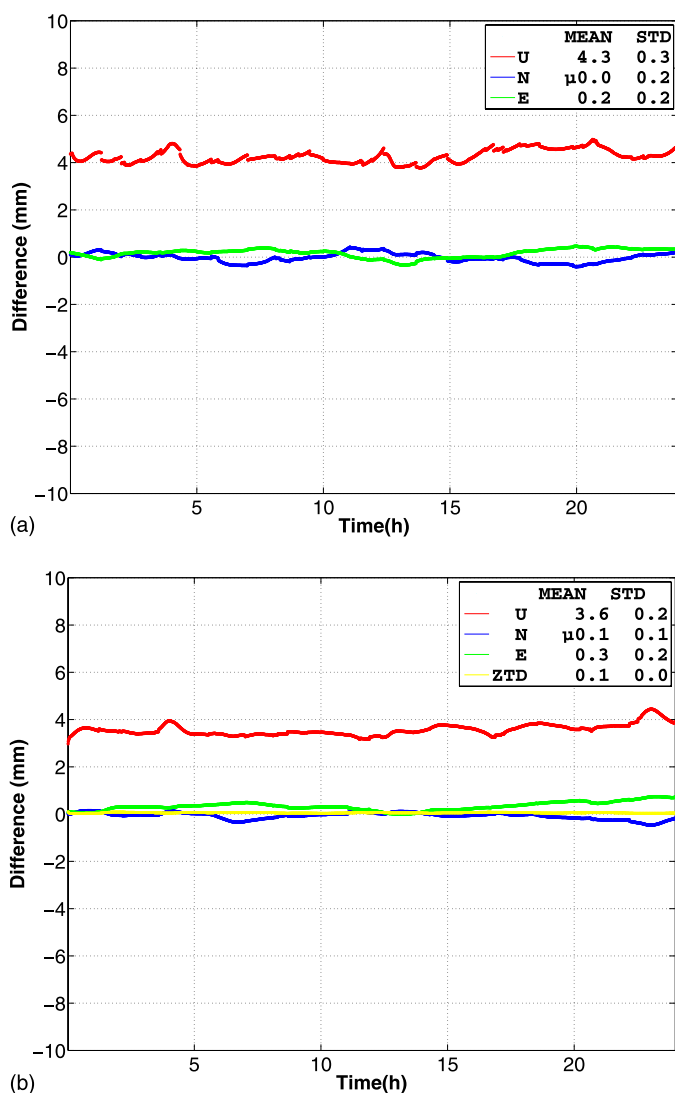


Fig. 6. (Color) (a) AMC2 single-frequency (GIM-corrected) N-E-U differences between using the GBC approach and RBC approach; and (b) AMC2 dual-frequency N-E-U and ZTD differences between using the GBC approach and RBC approach

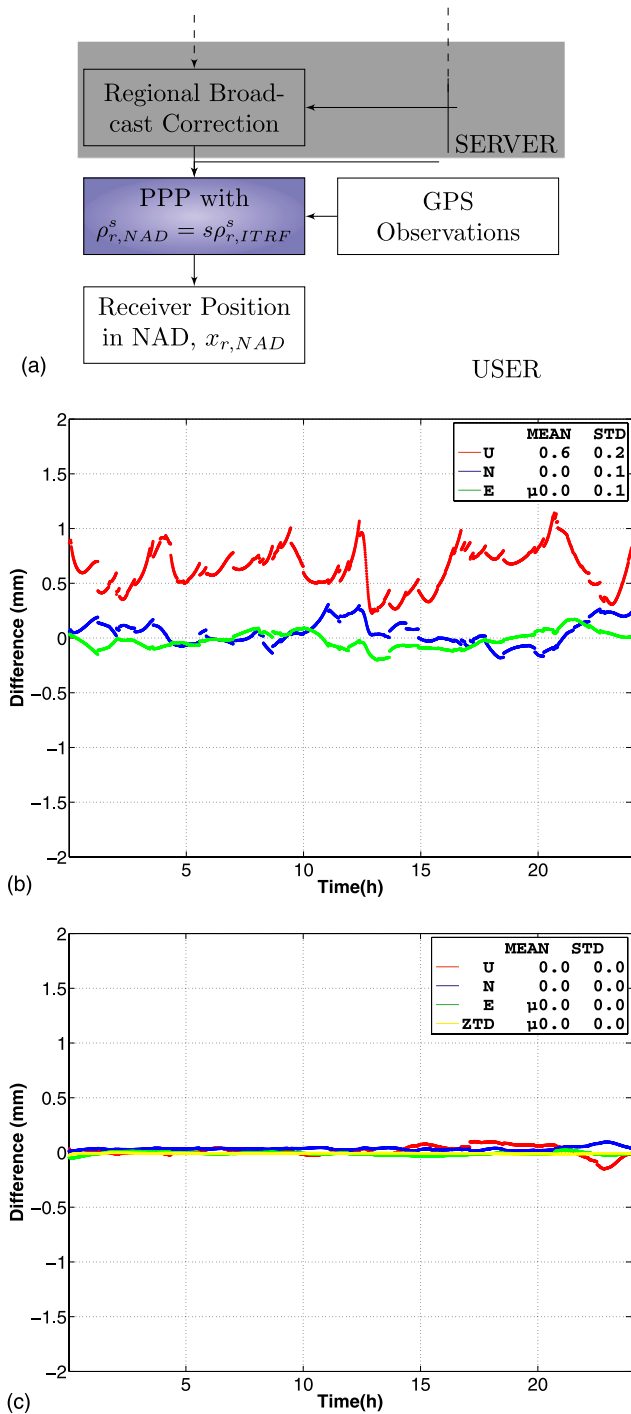


Fig. 7. (Color) (a) Location in the flow diagram of the modified RBC approach where the scale factor has to be applied; (b) AMC2 single-frequency (GIM-corrected) N-E-U differences between using the GBC approach and the modified, range-corrected, RBC approach (compare with Fig. 6); (c) AMC2 dual-frequency N-E-U and ZTD differences between using the GBC approach and the modified, range-corrected, RBC approach (compare with Fig. 6)

RBC approach are small, these differences are not zero. Hence, apart from the scale-induced bias, the RBC approach still contains other residual biases. Because these biases must have their origin, just like with the receiver-satellite range, in the usage of a different reference frame (GRF/ITRF versus RRF/NAD83), they can be traced by identifying the other components in the PPP model that are

reference frame choice dependent. This leads to the a priori corrections that are used in PPP; e.g., such as the corrections for tides, relativity, troposphere, and GIM. To analyze the significance of the reference frame choice dependency, the effect of having the required receiver and satellite positions in the a priori PPP corrections computed in NAD83 instead of in ITRF2005 was evaluated. As a result, it was found that among the a priori corrections the correction for the tropospheric delay stood out.

This also explains the difference between the single-frequency result of Fig. 7(b) and the dual-frequency result of Fig. 7(c). In the dual-frequency case the ZTD is estimated in both approaches. Hence, here the reference frame dependency is only felt in the receiver- and satellite-position dependency of the mapping function. Thus, the difference in the dual-frequency result of Fig. 7(c) is so small (less than 0.1 mm), because the mapping function of the GBC approach (evaluated in the ITRF) is practically identical to that of the RBC approach (evaluated in NAD83). In the single-frequency case, the difference between the two approaches is larger [cf. Fig. 7(b)] because now the tropospheric delay is a priori corrected for instead of being estimated.

Although the elimination of the residual biases in Figs. 7(b and c) requires, in principle, that all receiver position-dependent variables (latitude, height, and receiver-satellite elevation) of the a priori tropospheric correction be in the same reference frame, it was verified that the reference frame dependency of the tropospheric correction is primarily felt through the height variable. Hence, to eliminate the N-E-U differences between the GBC and RBC approaches it is sufficient to consider only the height variable and use same reference frame heights (e.g., both in ITRF) when evaluating the tropospheric correction in the two approaches. As previously mentioned, the height differences between ITRF2005 and NAD83(CORS96) are primarily a result of the nongeocentricity of NAD83(CORS96). Because the nongeocentricity of NAD83(2011) is of the same order, the previously described effect on the a priori tropospheric corrections will not change.

RT PPP with Unscaled RBCs

Instead of modifying the PPP algorithm, modifying the BCs can also be considered. By excluding the scale in the transformation of the orbital corrections the rather difficult to predict time-varying receiver-satellite geometry-dependent biases that are present in the current RBC approach can be avoided. By using RBCs that still have the scale of the GRF, the remaining biases become easy to predict and easy to correct for. Hence, with this approach, users will not have to modify their PPP algorithms. Instead, it then suffices to apply a simple a posteriori scale correction to the coordinates obtained with the unscaled-RBC approach.

Figs. 8 and 9 show the single- and dual-frequency results of applying the unscaled-RBC approach for Station AMC2 [note the difference in vertical axes scaling between Figs. 8(a and c) and Figs. 8(b and d), respectively, and between Figs. 9(a and c) and Figs. 9(b and d), respectively]. These results show that the a posteriori position vector scaling reduces the biases for single-frequency PPP (GIM corrected) to about 1 mm in height and that it practically eliminates the biases for dual-frequency PPP. Additionally, when the tropospheric correction is evaluated with the same height in the two approaches, the biases become completely eliminated.

Finally, it is shown that instead of using a posteriori position vector scaling for bias reduction or elimination, a simple constant a posteriori height correction may also be used. Recall from Eq. (8) that the first term on the right-hand side, Δsu , describes how the ellipsoidal coordinate differences are affected by scale. This term can be expressed in its components as

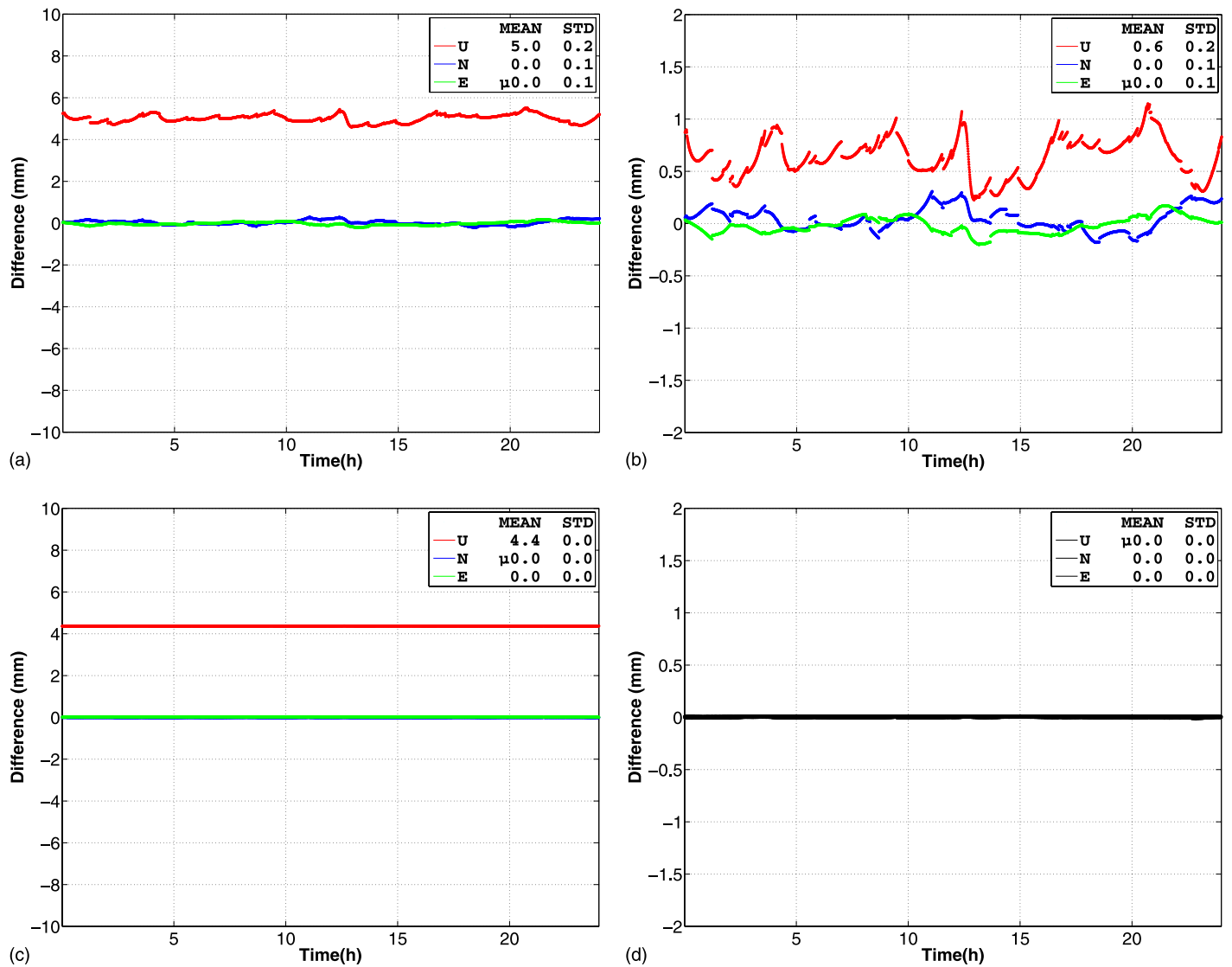


Fig. 8. (Color) AMC2 single-frequency (GIM-corrected) N-E-U differences between using the GBC approach and the unscaled RBC approach: (a and c) before and (b and d) after application of the a posteriori scale correction; (a and b) with the tropospheric correction in a different reference frame and (c and d) in the same reference frame (compare with Fig. 6)

$$\begin{bmatrix} \Delta h \\ (M + h)\Delta\phi \\ (N + h)\cos\phi\Delta\lambda \end{bmatrix} = \Delta s \begin{bmatrix} N(1 - e^2\sin^2\phi) + h \\ -Ne^2\sin\phi\cos\phi \\ 0 \end{bmatrix} \quad (11)$$

This shows that position vector scaling only affects the height and north-south components but not the east-west component as a result of the rotational symmetry of the ellipsoid. In fact, when applied to NAD83, also the north-south component can be discarded. This is shown in Fig. 10, which illustrates for the whole of North America the effect of the ITRF2005-NAD83 scale on the height and north-south components. This result also shows that the variation in the height differences can be discarded, and thus instead of using position vector scaling a single constant a posteriori height correction of 4.1 mm may as well be used. In the case of NAD83(2011), this correction becomes even smaller. It can be shown that with the IGS08-to-NAD83(2011) transformation (cf. Table 1), the height bias reduces to +1.8 mm for DOY 79 2011. This is because of the smaller scale difference of IGS08-NAD83(2011) compared with that of ITRF2005-NAD83(CORS96).

Summary and Conclusions

RT PPP requires RT precise corrections to broadcast orbits and clocks. These RT BCs are currently available in a GRF (the GBCs) as well as in RRFs (the RBCs). In this contribution, the PPP usage of the RBCs for positioning in the NAD83 was analyzed. GPS data from eight U.S. stations were collected and analyzed, thus enabling a PPP user coordinate-level comparison between the RBC approach and the traditional GBC approach. This was done for three different PPP variants, the single- and dual-frequency ionosphere-free variants and the single-frequency GIM-corrected variant.

The analysis demonstrated the limitations of the current RBC approach. Although the RBC approach is intended to produce positioning results in the regional datum, it does not provide results that are identical to the traditional GBC approach. These limitations are a result of the different reference frame usage in the two approaches (ITRF versus NAD83). These differences manifest themselves in the scale of the PPP receiver-satellite ranges and in the position dependency of the a priori PPP corrections, which in the case of

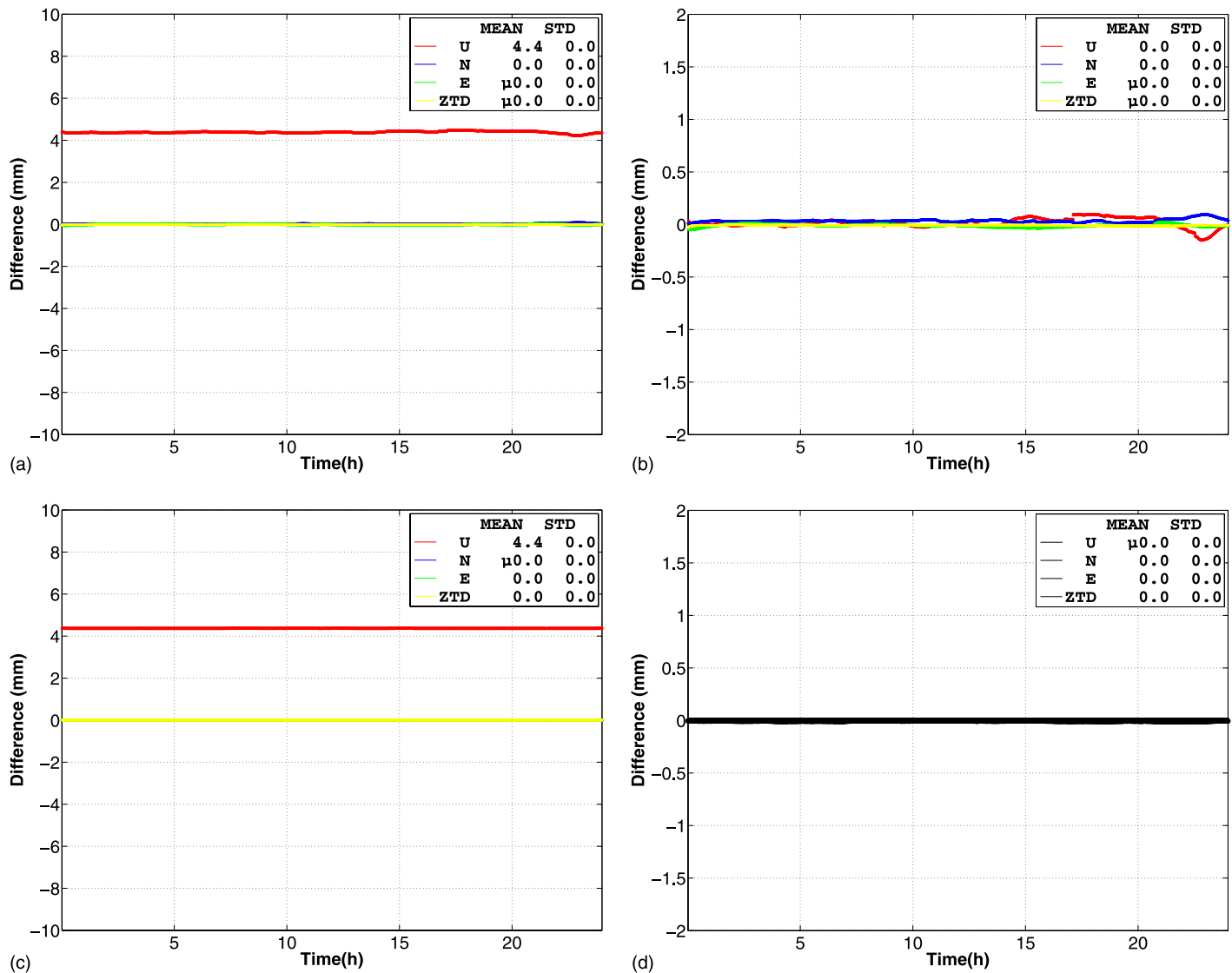


Fig. 9. (Color) AMC2 dual-frequency N-E-U differences between using the GBC approach and the unscaled RBC approach: (a and c) before and (b and d) after application of the a posteriori scale correction; (a and b) with the tropospheric correction in a different reference frame and (c and d) in the same reference frame (compare with Fig. 6)

NAD83 is primarily through the height dependence of the tropospheric correction.

It was shown that, depending on the PPP application at hand, various corrective actions can be taken. The difference between the two approaches is mainly felt in the height coordinate. Therefore, if the interest is only in two-dimensional horizontal positions and a time-fluctuating bias of less than a few mm is accepted, then no corrective action is needed. The same holds true for three-dimensional (3D) positions, if biases up to 0.5 cm are accepted.

Three approaches were described to reduce the differences in the height coordinate. Either the PPP algorithm for scale is modified, or RBCs that have the same scale as the GRF are used, followed by either an a posteriori position vector scaling or a simple constant height correction. As was shown, such corrective action is sufficient for dual-frequency PPP because it reduces the biases to a few tenths of a millimeter. For single-frequency PPP it may also be considered sufficient, provided that a remaining time-fluctuating height difference with the GBC approach of about 1 mm is accepted. Otherwise, the a priori tropospheric correction will have to be evaluated using the same reference frame height in both approaches.

For PPP-NAD83 practitioners the important conclusion is reached that the currently available RBC approach can still be used. Although an awareness of the inherent inconsistency with the traditional GBC approach is necessary, the NAD83 biases that the RBC usage generates are generally small compared with the achievable accuracy. Because the identified limitations of the RBC approach are a result of the different reference frame usage, these limitations will be resolved once the NGS plan to replace NAD83 with a new ITRF-aligned geometric datum is realized.

Acknowledgments

P.J.G. Teunissen is the recipient of an Australian Research Council (ARC) Federation Fellowship (Project No. FF0883188). Part of this work was done in the framework of Project 1.01 of the Cooperative Research Centre for Spatial Information (CRC-SI2). Observation data and broadcast corrections of the analysis have been made available by the Real-Time IGS Pilot Project. The North American digital terrain model was extracted from the global DTM2006.0

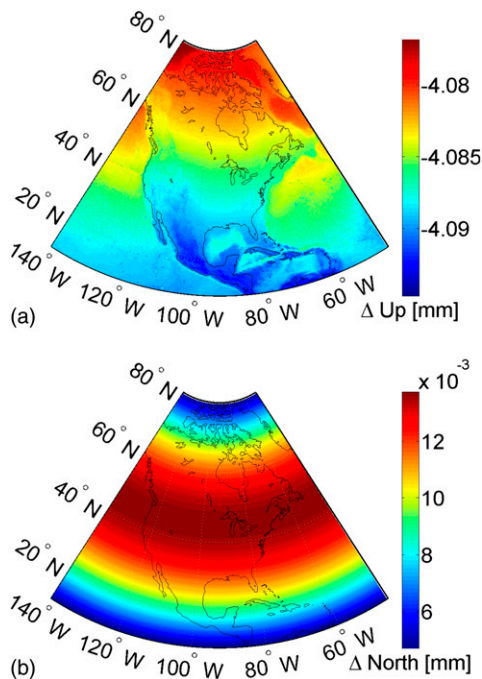


Fig. 10. (Color) (a) Height and (b) north-south correction when using the unscaled-RBC approach for NAD83 (Epoch DOY 079, 2011)

for this work by Dr. Christian Hirt. All of this support is gratefully acknowledged.

References

- Altamimi, Z., Collilieux, X., Legrand, J., Garayt, B., and Boucher, C. (2007). "ITRF2005: A new release of the International Terrestrial Reference Frame based on time series of station positions and earth orientation parameters." *J. Geophys. Res.*, 112(B9), 1–10.
- Bisnath, S., and Gao, Y. (2008). "Current state of precise point positioning and future prospects and limitations." *Observing our changing earth*, M. Sideris, ed., Vol. 133, Springer, Heidelberg, Germany, 615–623.
- Boucher, C., and Altamimi, Z. (1996). "International terrestrial reference frame." *GPS World*, 7(9), 71–74.
- Bundesamt für Kartographie und Geodäsie (BKG). (2010). "Real-time GNSS satellite orbit and clock corrections from IGS and EUREF sources." (<http://igs.bkg.bund.de/ntrip/orbits>).
- Center for Orbit Determination in Europe (CODE). (2006). (<http://www.aiub.unibe.ch/ionosphere.html>) (Jan. 18, 2012).
- Craymer, M. (2006). "The evolution of NAD83 in Canada." *Geomatica*, 60(2), 151–164.
- Craymer, M., Ferland, R., and Snay, R. (2000). "Realization and unification of NAD83 in Canada and the U.S. via the ITRF." *Proc., Int. Association of Geodesy Symp.*, Vol. 120, Springer, Heidelberg, Germany, 118–121.
- Davis, J., Herring, T., Shapiro, I., Rogers, A., and Elgered, G. (1985). "Geodesy by radio interferometry: effects of atmospheric modeling errors on estimates of baseline length." *Radio Sci.*, 20(6), 1593–1607.
- Hauschild, A., and Montenbruck, O. (2009). "Kalman-filter-based GPS clock estimation for near real-time positioning." *GPS Solutions*, 13(3), 173–182.
- Heroux, P., et al. (2004). "Products and applications for precise point positioning—Moving towards real-time." *Proc., ION GNSS ITM*, Institute of Navigation, Manassas, VA, 1832–1843.
- Ifadis, I. (1992). "The excess propagation path of radio waves: Study of the influence of the atmospheric parameters on its elevation dependence." *Surv. Rev.*, 31(243), 289–298.
- Kleijer, F. (2004). "Troposphere modeling and filtering for precise GPS leveling." *NCG Publications on Geodesy No. 56*, Nederlandse Commissie voor Geodesie, Delft, Netherlands.
- Kouba, J. (2002). "The GPS toolbox ITRF transformations." *GPS Solutions*, 5(3), 88–90.
- Kouba, J. (2003). "A guide to using international GPS service (IGS) products." (<http://igsceb.jpl.nasa.gov/igsceb/resource/pubs>) (Jan. 18, 2012).
- Kouba, J., and Heroux, P. (2001). "Precise point positioning using IGS orbit and clock products." *GPS Solutions*, 5(2), 12–28.
- Montenbruck, O. (2003). "Kinematic GPS positioning of LEO satellites using ionosphere-free single frequency measurements." *Aerosp. Sci. Technol.*, 7(5), 396–405.
- National Oceanic and Atmospheric Administration (NOAA). (2008). *The National Geodetic Survey ten-year plan: Mission, vision and strategy 2008–2018*, U.S. Dept. of Commerce, NOAA, Washington, DC., 1–55.
- National Oceanic and Atmospheric Administration (NOAA). (2011). "CORS coordinates." (<http://geodesy.noaa.gov/CORS/coords.shtml>) (Jan. 10, 2012).
- Niell, N. (1996). "Global mapping functions for the atmospheric delay at radio wavelengths." *J. Geophys. Res.*, 101(B2), 3227–3246.
- Ovstedal, O. (2002). "Absolute positioning with single frequency GPS receivers." *GPS Solutions*, 5(4), 33–44.
- Pavlis, N., Factor, J., and Holmes, S. (2006). "Terrain-related gravimetric quantities computed for the next EGM." *Proc., 1st Int. Symp. of the Int. Gravity Field Service*, Springer, Heidelberg, Germany, 318–323.
- Pearson, C., McCaffrey, R., Elliott, J., and Snay, R. (2010). "HTDP 3.0: Software for coping with the coordinate changes associated with crustal motion." *J. Surv. Eng.*, 136(2), 80–90.
- Petit, G., and Luzum, B. (2010). "IERS conventions 2010." (<http://maia.usno.navy.mil/conv2010/tn36.pdf>) (Jan. 18, 2012).
- Rebischung, P., Schmid, R., and Ray, J. (2011). "Upcoming switch to IGS08/igs08.atx, IGSMAIL-6354." (<http://igsceb.jpl.nasa.gov/pipermail/igsmail/2011/006346.html>) (Jan. 10, 2012).
- Saastamoinen, J. (1972a). "Contributions to the theory of atmospheric refraction." *Bull. Geod.*, 105(1), 279–298.
- Saastamoinen, J. (1972b). "Introduction to practical computation of astronomical refraction." *Bull. Geod.*, 106(1), 383–397.
- Saastamoinen, J. (1973). "Contributions to the theory of atmospheric refraction. Part II: Refraction corrections in satellite geodesy." *Bull. Geod.*, 107(1), 13–34.
- Schaer, S. (1999). "Mapping and predicting the earth's ionosphere using the global positioning system." Ph.D. thesis, Univ. of Berne, Berne, Switzerland.
- Schwarz, C. E. (1989). "North American Datum of 1983." *NOAA Professional Paper No. 2*, National Oceanic and Atmospheric Administration, Washington, D.C.
- Snay, R., and Soler, T. (2000a). "Modern terrestrial reference systems. Part 2: The Evolution of NAD83." *Prof. Surv.*, 20(2), 16–18.
- Snay, R., and Soler, T. (2000b). "Modern terrestrial reference systems. Part 3: WGS 84 and ITRF." *Prof. Surv.*, 20(3), 1–3.
- Sohne, W. (2010). "EPN special project real-time analysis status report." (<http://www.euref-iag.net/TWG/EUREF/b-euref2010-realtime-soehne.pdf>) (Jan. 18, 2012).
- Sohne, W., Sturze, A., and Weber, G. (2008). "Enhancement of EPN real-time data streams." (<http://www.epncb.oma.be/organisation/projects/RTanalysis/enhancement-realtime.pdf>) (Jan. 18, 2012).
- Soler, T., and Marshall, J. (2003). "A note on frame transformations with applications to geodetic datums." *GPS Solutions*, 7(1), 23–32.
- Soler, T., and Snay, R. (2004). "Transforming positions and velocities between the International Terrestrial Reference Frame of 2000 and North American Datum of 1983." *J. Surv. Eng.*, 130(2), 49–55.
- Tetreault, P., Kouba, J., Heroux, P., and Legree, P. (2005). "CSRS-PPP: An internet service for GPS user access to the Canadian spatial reference frame." *Geomatica*, 59(1), 17–28.
- van Bree, R. J. P., and Tiberius, C. C. J. M. (2012). "Real-time single-frequency precise point positioning: Accuracy assessment." *GPS Solutions*, 16(2), 259–266.
- Weber, G., Mervart, L., Lukes, Z., Rocken, C., and Dousa, J. (2007). "Real-time clock and orbit corrections for improved point positioning via NTRIP." *Proc., ION GNSS*, Institute of Navigation, Manassas, VA, 1992–1998.
- Zumberge, J., Hefflin, M., Jefferson, D., Watkins, M., and Webb, F. (1997). "Precise point positioning for the efficient and robust analysis of GPS data from large networks." *J. Geophys. Res.*, 102(B3), 5005–5017.